Mutual Coupling Compensation-based Nonuniform Fourier Transform Technique for Accurate and Efficient Pattern Evaluation and its Application to Synthesis of Aperiodic Arrays

Fan Peng[1], Cheng Liao[1], You-Feng Cheng[1], Ju Feng[1], and Si-Du Wang[2]

[1]Institute of Electromagnetics
Southwest Jiaotong University, Chengdu, 610031, China
pfan2023@my.swjtu.edu.cn, c.liao@swjtu.edu.cn, juvencheng@swjtu.edu.cn, fengju-fj@swjtu.edu.cn

[2]Mianyang Flight College of Civil Aviation
Flight University of China, Mianyang, 621000, China
1075972066@qq.com

Abstract – A rapid solution for evaluating the radiation pattern of aperiodic arrays, taking into account mutual coupling, is presented in this paper. The evaluation is achieved by eliminating the anisotropy of the active element pattern of the array through the use of the mutual coupling compensation matrix (MCCM) technique, in conjunction with the non-uniform fast Fourier transform (NuFFT). In order to eliminate the impact of mutual coupling on array pattern calculation, the MCCM is utilized to convert the active element pattern (AEP) of each element into a shared uniform term and make the NuFFT technique suitable for the array pattern calculation. The proposed solution is validated by evaluating the radiation pattern of a 64-element planar aperiodic array. In addition, the proposed solution is integrated into the Particle Swarm Optimization (PSO) to realize a pattern synthesis method. Two synthesized patterns, including a pencil beam with low sidelobe level and a flat-top beam pattern, are executed to validate. Compared with several reported methods, the proposed method can improve the synthesis efficiency and maintain good accuracy simultaneously.

Index Terms – aperiodic array, mutual coupling compensation, non-uniform fast Fourier transform, radiation pattern calculation and synthesis.

I. INTRODUCTION

Compared with periodic arrays, aperiodic arrays have attracted much attention in recent years because of several excellent advantages, such as suppression of grating lobes, reduction of cost and high degree of freedom in design [1]. However, the diversity of mutual coupling (MC) introduced by the aperiodic layout results in inaccurate evaluation of the radiating pattern. Besides, due to the aperiodic layout, some efficient synthesis solutions, such as the iterative Fourier transform (IFT) technique [2], are no longer applicable. In published literature, the aperiodic array is usually transformed to a periodic one by embedding an amount of virtual elements to realize the accurate evaluation and fast synthesis. In [3], a virtual uniform array is established, and the element in the real aperiodic array is interpolated by several adjacent elements in the virtual one. In this situation, it is convenient to realize the fast synthesis of the aperiodic array by applying the IFT technique. However, the MC is not considered in the synthesis. You, et al. [4] proposed a concept of active element pattern expansion (AEPE) method and realized the fast synthesis of uniformly-spaced linear array. Inspired by the above AEPE and virtual uniform array, Liu, et al. [5] further presented a novel virtual active element pattern expansion method (VAEPE) and integrated it with the IFT procedure, resulting in a fast synthesis of aperiodic arrays including the MC. Nevertheless, these methods often dramatically increase the size strong of the array, which results in high complexity.

In contrast to the above methods, the fast synthesis of aperiodic arrays also can be directly accomplished by the non-uniform fast Fourier transform (NuFFT) technique [6–10]. The NuFFT technique, in which a variety of uniform sampling with a denser grid is generated, is the expansion of the fast Fourier transform (FFT) technique [11–14]. The time complexity of pattern evaluation is reduced successfully to $O(N \log N)$ from $O(N^2)$. Therefore, it can be integrated into many pattern synthesis methods, such as the stochastic optimization algorithms [15, 16], convex optimization technique [17] and other solutions [18–20] to improve the synthesis efficiency. In [15], the NuFFT technique based on Gaussian interpolation is chosen to reduce optimization time of the aperiodic array. However, those methods are only suitable for the ideal array, which means each element of the

array is seen as an isotropic source and MC is not taken into consideration. In fact, the MC has crucial influences on the radiation pattern of aperiodic array, especially when patterns with low sidelobe level (SLL) and specific nulls are required. To date, realizing the accurate evaluation and fast synthesis of aperiodic arrays is still a strong challenge in the area of phased arrays.

In this paper, an improved NuFFT-based solution to calculate and synthesize the far-field pattern of arbitrary aperiodic arrays is proposed and analyzed. Firstly, the mutual coupling compensation matrix (MCCM) [21–23] is utilized to approximate each active element pattern (AEP) to a far-field pattern of the array without the consideration of MC with compensated excitation. On this basis, the isolated element pattern (IEP) can be extracted outside of the summation of the array pattern. Then, the NuFFT is introduced to form a novel fast pattern evaluation method and accelerate the calculation process. A numerical example of a 64-element planar aperiodic array is chosen to validate the proposed solution. Afterwards, the above solution is integrated into Particle Swarm Optimization (PSO) to replace the conventional pattern multiplication method (PMM) for the radiation pattern synthesis of aperiodic arrays. Two synthesized patterns including a pencil beam with low sidelobe level and a flat-top beam pattern of two linear aperiodic arrays are realized with amplitude and phase weighting, which results indicate that the proposed method can improve the synthesis efficiency and maintain high accuracy simultaneously compared with several reported methods.

II. MC COMPENSATION-BASED NUFFT TECHNIQUE

Without loss of generality, let us consider a planar array composed of N elements which are arbitrarily located in the xoy-plane. The position of the n-th element is denoted as (x_n, y_n). If MC or edge effect is neglected, the ideal radiation pattern (IRP) of the array can be described as the product of the array factor (AF) and IEP by PMM:

$$
\begin{aligned}
P_i(\theta, \varphi) &= E_{i0}(\theta, \varphi) \cdot \left(\sum_{n=1}^{N} w_i^n e^{jk(x_n u + y_n v)} \right) \\
&= \sum_{n=1}^{N} w_i^n \left(E_{i0}(\theta, \varphi) e^{jk(x_n u + y_n v)} \right) \\
&= \mathbf{E}_i \mathbf{W}_i,
\end{aligned}
\tag{1}
$$

with

$$
\mathbf{E}_i = \begin{bmatrix} E_{i0}(\theta, \varphi) e^{jk(x_1 u + y_1 v)} \\ \vdots \\ E_{i0}(\theta, \varphi) e^{jk(x_N u + y_N v)} \end{bmatrix}^T \quad \mathbf{W}_i = \begin{bmatrix} w_i^1 \\ \vdots; \\ w_i^N \end{bmatrix}, \tag{2}
$$

where w_i^n is the n-th ideal element excitation of the array, E_{i0} is the IEP of the array element, k is the free space

wavenumber at operation frequency, $u = \sin\theta\cos\varphi$, $v = \sin\theta\sin\varphi$ separately and (θ, φ) are the observation direction defined by standard spherical coordinate, the notation "$(\cdot)^T$" is the transpose operator. It is apparent that the Fourier transform-pair relationship exists between AF and array excitation, which means $P_i(\theta, \varphi)$ can be calculated quickly by using the NuFFT technique.

On the contrary, when the MC effect is taken into consideration, the actual radiation pattern (ARP) of the array $P_r(\theta, \varphi)$ can be given by the AEP method (AEPM) [24] as follows:

$$
\begin{aligned}
P_r(\theta, \varphi) &= \sum_{n=1}^{N} w_r^n E_r^n(\theta, \varphi) \\
&= \mathbf{E}_r \mathbf{W}_r,
\end{aligned}
\tag{3}
$$

with

$$
\mathbf{E}_r = \begin{bmatrix} E_r^1(\theta, \varphi) \\ \vdots \\ E_r^N(\theta, \varphi), \end{bmatrix}^T \quad \mathbf{W}_r = \begin{bmatrix} w_r^1 \\ \dots \\ w_r^N \end{bmatrix}, \tag{4}
$$

where w_r^n is the actual excitation of the n-th element, E_r^n is the AEP corresponding element n. Note that all of the array elements are placed in a common and unique coordinate system. Because of the MC of the array, the AEPs are different from each other, which results in the calculation of $P_r(\theta, \varphi)$ only relying on the summation of AEPs of all elements. In this case, the NuFFT technique is not applicable.

In general, the pattern is evaluated by formula (1) in the pattern synthesis program. After being synthesized, the excitation $\mathbf{W}_i$ is used in the real array analysis. It is obvious that a distorted radiation pattern $P_r(\theta, \varphi)$ with respect to the ideal synthesized pattern $P_i(\theta, \varphi)$ is obtained. Therefore, a method to make the IRP fit to the ARP in whole space and which has the ability to use the FFT/NuFFT technique is needed. To this end, the MCCM is introduced.

The method for solving MCCM of uniform arrays had been reported in [22], and it is further introduced and improved here for non-uniform arrays. Specifically, for the purpose of making the ARP $P_r(\theta, \varphi)$ and the IRP $P_i(\theta, \varphi)$ as similar as possible, the least square method is adopted, the maximum similarity between $P_r(\theta, \varphi)$ and $P_i(\theta, \varphi)$ can be expressed as:

$$
\min \iint |P_r(\theta, \varphi) - P_i(\theta, \varphi)|^2 \sin\theta \, d\theta \, d\varphi, \tag{5}
$$

the above integration will be carried out in visible space to obtain a minimum mean square error and can be rewritten into the following matrix form:

$$
\min_{\mathbf{W}_i} \mathbf{W}_r^H \mathbf{Q} \mathbf{W}_r - \mathbf{W}_i^H \mathbf{P}^H \mathbf{W}_r - \mathbf{W}_r^H \mathbf{P} \mathbf{W}_i + \mathbf{W}_i^H \mathbf{C} \mathbf{W}_i,
\tag{6}
$$

where $\mathbf{Q}$, $\mathbf{P}$ and $\mathbf{C}$ all are $N \times N$ matrices, which can be calculated by the following formulas:

$$\mathbf{Q} = \iint \mathbf{E}_r^H \mathbf{E}_r \sin\theta d\theta d\varphi,$$

$$\mathbf{P} = \iint \mathbf{E}_r^H \mathbf{E}_i \sin\theta d\theta d\varphi, \qquad (7)$$

$$\mathbf{C} = \iint \mathbf{E}_i^H \mathbf{E}_i \sin\theta d\theta d\varphi.$$

Furthermore, the solution of (6) is derived as:

$$\mathbf{W}_i = \mathbf{P}^{-1} \mathbf{Q} \mathbf{W}_r. \qquad (8)$$

Thus, the MCCM $\mathbf{C}$ is written as:

$$\mathbf{C} = \mathbf{P}^{-1} \mathbf{Q}. \qquad (9)$$

Since $\mathbf{C}$ defines a relation between $\mathbf{W}_r$ and $\mathbf{W}_i$, the compensated excitation enables the calculated array pattern in (1) to maintain the maximum approximation to the ARP. In this situation, $P_r(\theta, \varphi)$ can be easily rewritten as:

$$P_r(\theta, \varphi) = \mathbf{E}_r \mathbf{W}_r \approx \mathbf{E}_i \mathbf{W}_i = \mathbf{E}_i (\mathbf{C} \mathbf{W}_r), \qquad (10)$$

where $\mathbf{C} \mathbf{W}_r$ is seen as the compensated excitation. It can be seen from (10) that the consideration of MC is shifted from AEPs to excitation term which is easier to deal with. The reason why the symbol '$\approx$' holds is that the least squares equation in (5) just merely guarantees the approximation. Note that the approximation is able to provide the sufficient computational accuracy, which can be proved by the subsequent comparisons between the results of the numerical calculation and full-wave simulation. Substituting (10) for (1), the approximation of ARP would be easily achieved and given by:

$$P_r(\theta, \varphi) \approx E_{i0}(\theta, \varphi) \cdot \sum_{n=1}^{N} \left(\sum_{m=1}^{N} c_{nm} w_r^m e^{jk(x_m u + y_m v)} \right), \qquad (11)$$

where the c_{nm} is the (n, m)-th term of $\mathbf{C}$. This term represents the compensation of m-th element on the n-th element of array due to the coupling. It can be observed from (10) and (11) that the calculation of $P_r(\theta, \varphi)$ is replaced by the calculation of $P_i(\theta, \varphi)$ with excitation $\mathbf{C} \mathbf{W}_r$, and the far-field calculation obeys the principle of pattern multiplication again. In other words, the ARP $P_r(\theta, \varphi)$ can be represented by the IEP and the AF, the AF here is:

$$AF = \sum_{n=1}^{N} \left(\sum_{m=1}^{N} c_{nm} w_r^m e^{jk(x_m u + y_m v)} \right). \qquad (12)$$

Obviously, the Fourier transform-pair relationship exists between AF and compensated excitation $\mathbf{C} \mathbf{W}_r$, therefore the NuFFT technique can be applied to accelerate the calculation. In addition, when w_r^n in (11) equals 1, the AEP of the n-th array element $E_r^n(\theta, \varphi)$ is approximated by:

$$E_r^n(\theta, \varphi) \approx E_{i0}(\theta, \varphi) \cdot \left(\sum_{m=1}^{N} c_{nm} e^{jk(x_m u + y_m v)} \right). \qquad (13)$$

From (13), the AEP of each element can be seen as a synthesized pattern with excitation of $c_{n,1:N}$. The time complexity of the PMM in (1) is $O(MN)$, and that of (11) drops to $O(MlogM)$ by introducing the NuFFT with M sampling points [10]. In this way, the efficiency of the calculation of $P_r(\theta, \phi)$ is significantly enhanced.

An example is provided to verify the effectiveness of the MCCM-NuFFT solution. A two-dimensional (2-D) planar array, which is composed of 64 rectangle patch antenna shown in Fig. 1 (a) and operates at 5 GHz, is selected and the array layout is drawn in Fig. 1 (b). Figure 2 shows the comparison between the AEP and the approximative element pattern of the center element (29-th) obtained by Ansys HFSS and MCCM-NuFFT solution respectively, the IEP of the antenna element is given simultaneously. As observed, the AEP is quite different with the IEP due to the MC, a serious distortion about 5 dBV/m of E-field generated in the broadside direction from the Fig. 2 (b). In addition, the main beam direction has been changed. On the contrary, the approximative element pattern obtained by the MCCM-NuFFT method is nearly similar to the original AEP, which can fit well the curve of the original AEP in most angular ranges. Only when θ is greater than $80°$ do the difference of the
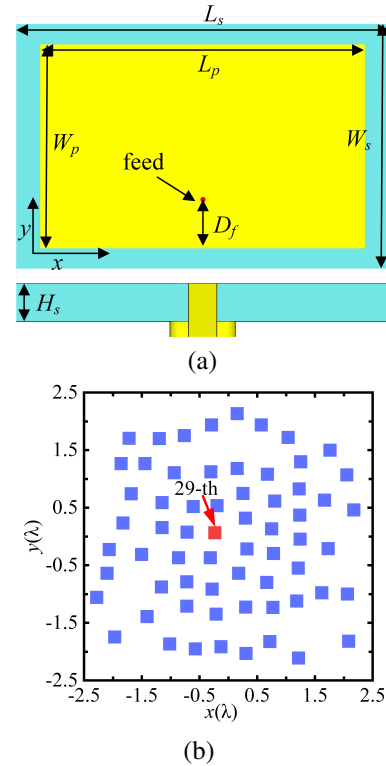

(a)

(b)

Fig. 1. (a) The geometry of the antenna element. (b) The array layout. (b) W_s=27.6 mm, L_s=22.08 mm, W_p=23 mm, L_p=18.4 mm, D_f=6 mm, H_s=2 mm.
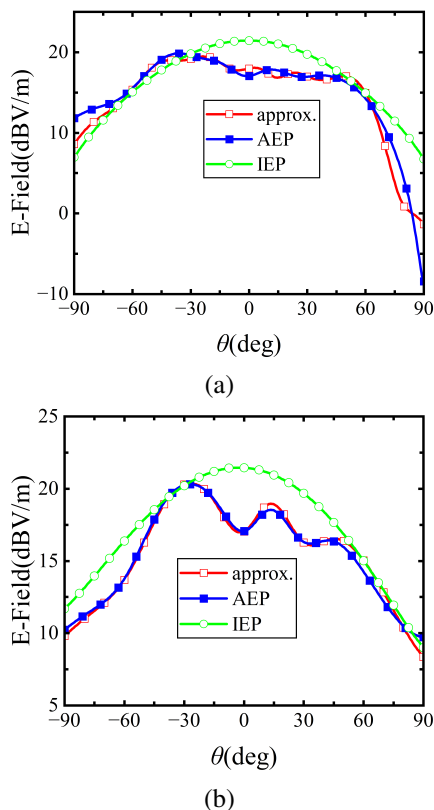
(a)

(b)

Fig. 2. The compensated pattern of 29-th element (a) *xoz*-plane, (b) *yoz*-plane.
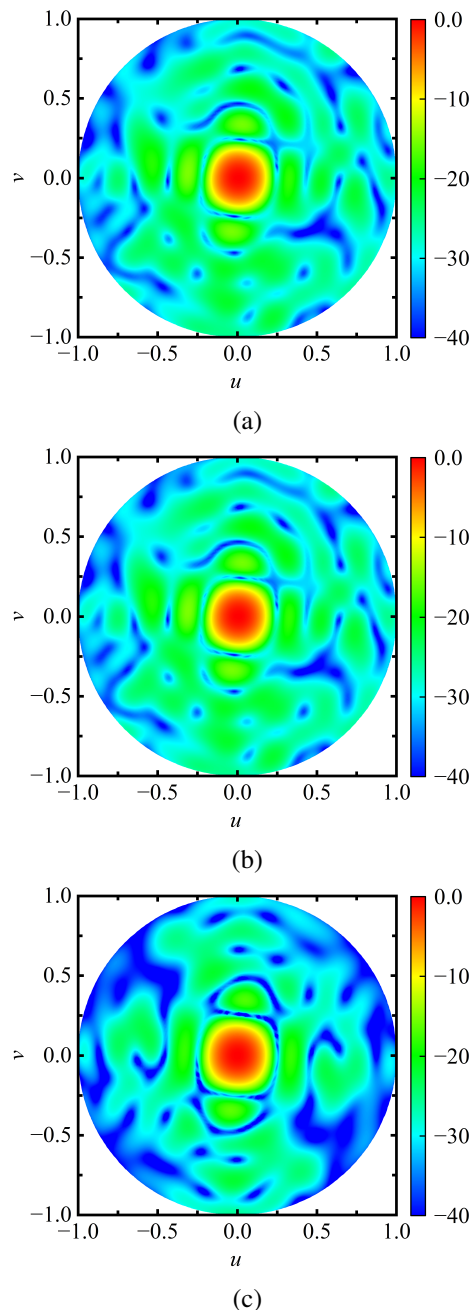

(a)

(b)

(c)

Fig. 3. The normalized radiated pattern of planar 64-element 2-D planar array with different methods, (a) pattern based on Ansys HFSS, (b) pattern based on MCCM-NuFFT, (c) pattern based on PMM.

curves slightly increase. Figure 2 demonstrates that the distortion pattern of the array element caused by the MC can be compensated well by the MCCM.

In addition, Fig. 3 illustrates the top view of the 3D normalized radiating pattern of the aperiodic array using several methods. Figure 4 provides the 2D patterns of both the *xoz* and *yoz* planes. The simulated pattern obtained by Ansys HFSS in Fig. 3 (a) serves as a benchmark to compare the accuracy of the two methods. As observed in Fig. 3 (b), the pattern generated by the MCCM-NuFFT method closely matches the simulated result. The main performance parameters of the array, such as the realized gain and peak sidelobe level (PSL), agree well with the simulated values. Only minor deviations exist in the high-elevation area. This discrepancy can be attributed to the fact that the approximation is conducted across the entire space. Consequently, errors of the same magnitude can manifest as larger relative differences in smaller simulated results expressed in decibels (dB) [25]. Conversely, the pattern obtained by the PMM method exhibits greater differences. While good approximation is maintained in the mainbeam area, noticeable discrepancies arise in the sidelobe regions. Additionally, the 2D pattern in Fig. 4 reveals a degradation in sidelobe

levels of up to 5 dB, along with changes in null positions. It is evident that the lack of consideration for mutual coupling is the reason behind these discrepancies. These results demonstrate that the proposed method effectively incorporates mutual coupling in the evaluation process of the array pattern.
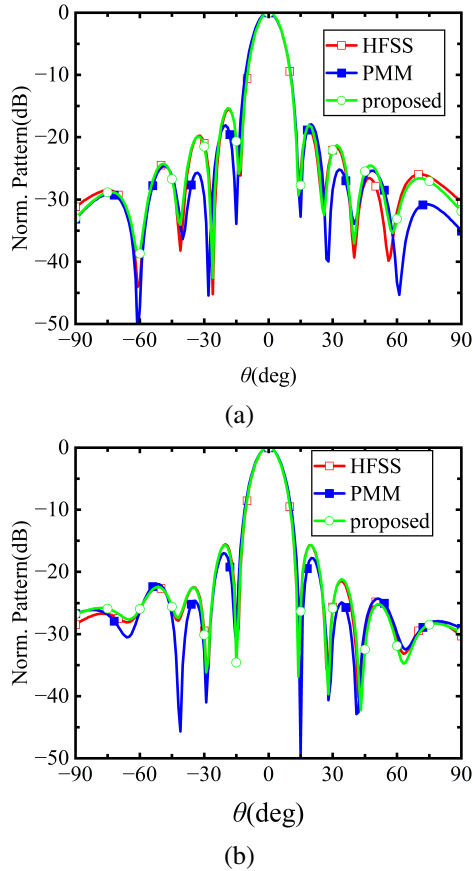
(a)

(b)

Fig. 4. The normalized 2D radiating pattern of 64-element 2-D planar array in different methods, (a) *xoz*-plane, (b) *yoz*-plane.
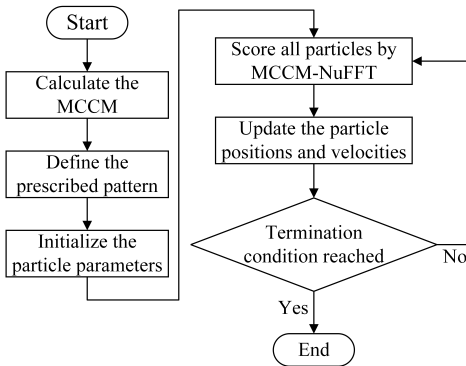

Fig. 5. The flowchart of proposed synthesis method.

III. FAST SYNTHESIS AND VALIDATION
A. Description of synthesis method

Based on the superiority of efficiency and accuracy, the MCCM-NuFFT method is integrated into the PSO to form a synthesis procedure in this section. The PSO algorithm has been applied to different electromagnetic applications such as array pattern synthesis [26, 27], and antenna design [28] because of the flexible constraints and its robustness to real-world problems. The corresponding flowchart is shown in Fig. 4, a brief description of this procedure is shown as follows:

a) Calculate MCCM **C**: obtain the AEP and the IEP of the predefined array by simulation or measurement. The MCCM **C** can be calculated by the method presented in section II and the reference [22].

b) Define the prescribed pattern: define the mainlobe region, sidelobe region, and PSL. If the target pattern is a shaped pattern, the lower and upper boundaries of the shaped region must be set up.

c) Initialize the particle position vector X of Q random individuals for amplitude-phase optimization. A set of random velocities V is also initialized between v_{min} and v_{max}.

d) Score all particles: evaluate the pattern including MC effect of each particle using the above MCCM-NuFFT method. Record the global optimal particle p_g and local optimal particles P_l of each particle separately.

e) Update the positions and velocities of particles.

f) Check if the optimal pattern meets the requirement. If yes, the synthesis procedure would be stopped, or go back to step (d) before going up to the maximum iteration number.

It is obvious that the fitness value of each particle corresponding to a solution must be evaluated in the iteration process. Therefore, equation (1) based on PMM needs QMN complex summations while the proposed MCCM-NuFFT method only requires $QMlogM$ because the NuFFT is available. This means the cost time is significantly saved while the accuracy can be maintained simultaneously. Two pattern synthesis examples are executed to verify the performance improvement on efficiency and accuracy of the proposed modified PSO method.

B. Focused beam pattern synthesis

In the first example, a focused beam of a 16-element linear array with reduced sidelobe is synthesized. The proposed modified PSO method and the PSO solution in [26] are compared to synthesize the same pattern simultaneously by optimizing the excitation amplitudes and phases. For the proposed method, the array element is assumed to be the microstrip antenna shown in Fig. 1 (a), while the array element is set as the isotropic source in the PSO method. The element positions and excitations are given in Fig. 6. The synthesized patterns of the proposed modified PSO method and the PSO solution in [26] are both shown in Fig. 7.
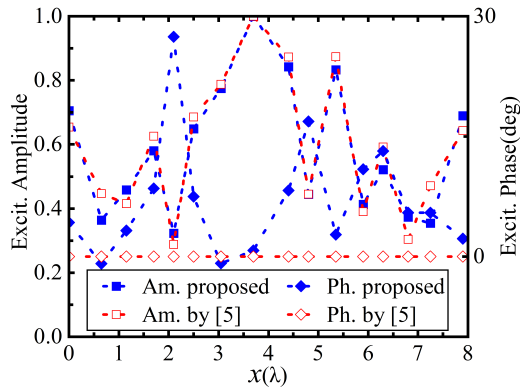
Fig. 6. The optimized excitation of 16-element linear array by two methods.
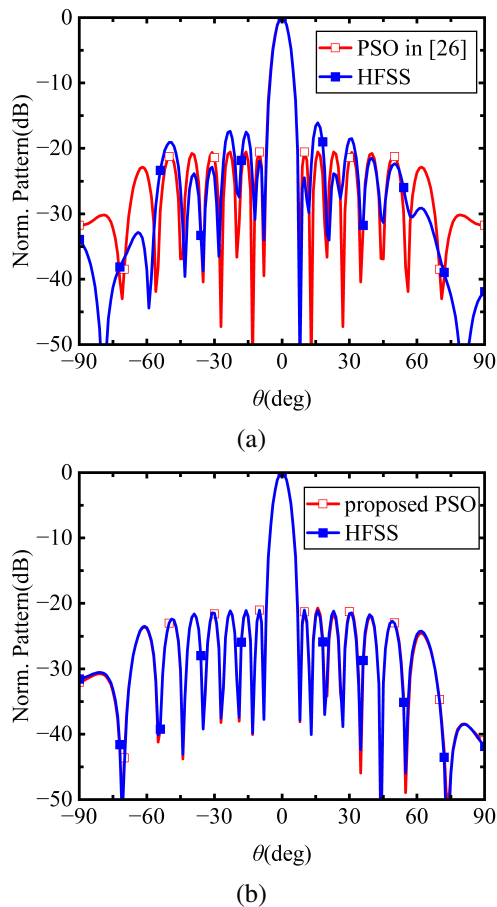

(a)

(b)

Fig. 7. The normalized pattern of 16-element linear array by (a) PSO in [26] and (b) proposed modified PSO method.

As can be seen, sidelobe levels lower than -21 dB are both obtained by two synthesized methods. However, when excitation amplitudes and phases are applied

to the 16-element array, significant deteriorations occur on the corresponding simulated pattern shown in Fig. 7 (a), the PSL reaches to -16 dB and the simulated pattern in the high-elevation areas vary sharply compared to the synthesized one. That means the solution reported in [26] may encounter some difficulties when it is used to synthesize a scanning beam. By contrast, the difference between patterns realized by the proposed method can be neglected. As plotted in Fig. 7 (b), the PSL remains as -21 dB. It is noted that the accurate synthesized pattern can also be obtained by AEPM. However, the calculation time would be increased because AEPs of array elements are quite different, which results in low synthesis efficiency. Besides, the subsequent time-consuming analysis also proves this point.

C. Flat-top beam pattern synthesis

A numerical experiment is performed and analyzed here to show the superiority in accuracy and efficiency of the proposed synthesis procedure. The experiment is going to synthesize a flat-top beam pattern of a linear aperiodic array composed of 12 dipole antennas by using amplitude-phase optimization, the dipole which works at central frequency of 1 GHz is designed to have a length of 144 mm and a radius of 1.5 mm. The desired pattern was achieved previously in [29] with the aperiodic array composed of 12 isotropic elements by the forward-back matrix pencil method. Then, the similar pattern including MC effect was also realized in [5] by utilizing the IFT method based on the VAEPE method.

The optimized compensated excitation, including the amplitudes and phases, are shown in Fig. 8, the corresponding actual excitation transformed by MCCM is also given. It reveals that the compensated excitation is similar to the actual ones. The difference of excitation amplitudes only emerges on elements on either sides, and the amplitudes of middle elements basically remain unchanged. In terms of excitation phases, they all differ from the original excitation ones. This phenomenon
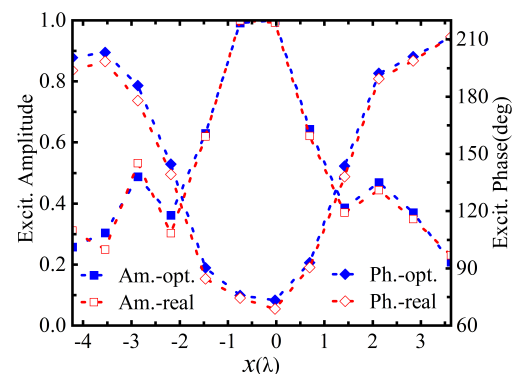

Fig. 8. The optimized and actual excitation.

suggests that excitation phases derive more influences of MC in this synthesis.

The synthesized patterns are shown in Fig. 9 which also includes patterns obtained by real AEPs and the solutions reported in [5] and [29]. It is obvious that all synthesized patterns obtained by these methods fully satisfy the pre-defined constraints. However, the corresponding simulated pattern, which is obtained when the optimized excitation given in [29] applies to the practical
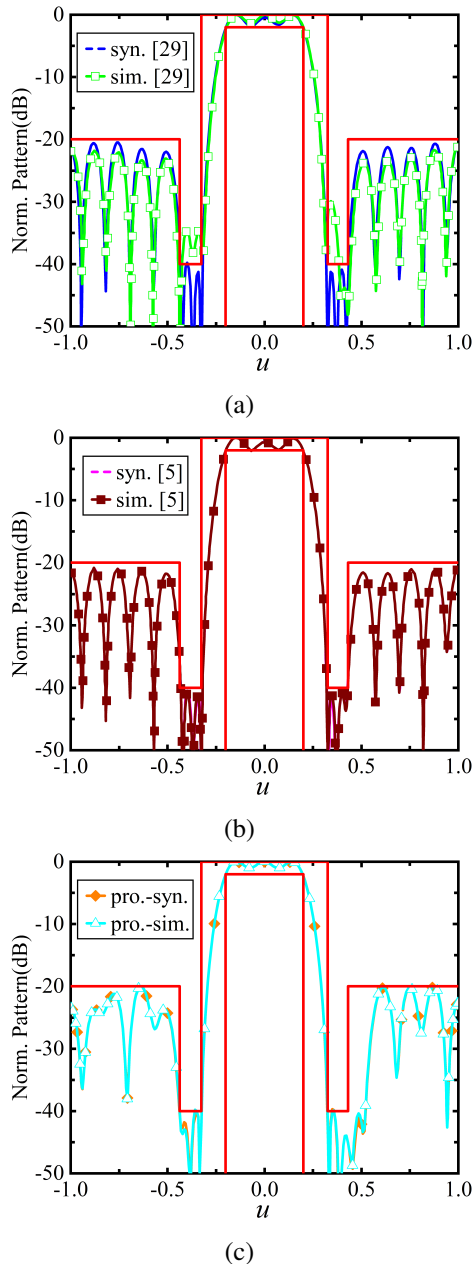

(a)

(b)

(c)

Fig. 9. The flat-top beam patterns of the 12-element dipole array obtained by several solutions, (a) result from [29], (b) result from [5], (c) result from proposed.

array, has some deterioration when compared with the synthesized one, especially in the -40-dB null regions. This indicates that the synthesized excitation obtained by common optimization cannot achieve the desired pattern with the actual array design. In terms of the pattern obtained by the proposed procedure, it can be seen that the synthesized pattern has a good agreement with the simulated result, which demonstrates that the MC effect can be considered well during the synthesis. Good agreement is also obtained between the synthesized pattern and the actual one with the optimized excitation in [5]. Nevertheless, the virtual array excitation of each real AEP requires a matrix inverse operation, which is time consuming, resulting in the high complexity of the VAEPE method.

Furthermore, the computational time of the proposed solution represented in Table 1 is recorded to analyze the efficiency improvement as well as the results based on the AEPM defined in (2). It should be noted that, since patterns obtained by PMM are not accurate enough, two methods including AEPM and the proposed MCCM-NuFFT are compared and analyzed here. All numerical computations are carried out by 100 trials on an Intel(R) Core (TM) i5-8600k 3.6 GHz CPU, 16 GB RAM computer with MATLAB platform. From Table 1, the computational time of the proposed solution shows some advantages. For instance, when the 64-element 2-D planar array in section II is selected, the computational time of the MCCM-NuFFT solution only takes 0.56 s while the AEPM of (2) requires 4.98 s with 256×256 spatial sampling points. In addition, the computational time quickly grows with the number of spatial sampling and array size for the AEPM. That means the advantages would be magnified synchronously with the increase of the number of the spatial sampling and array size. A similar conclusion can be obtained in other related literature about NuFFT.

Finally, the computational time of the method in [5] is negligible due to the introduction of the FFT. Nevertheless, the indispensable calculation of related coefficients greatly reduces the efficiency of the algorithm. For example, when the example of 64-element 2-D planar

Table 1: The computational time of proposed method and AEPM (unit: s)

Array Type		Sampling Number			
		256	512	1024	2048
12-ele. array	AEPM	0.0102	0.0145	0.0173	0.0371
	Proposed	0.0113	0.0124	0.0156	0.022
16-ele. array	AEPM	0.0131	0.0178	0.0216	0.0457
	Proposed	0.0127	0.0131	0.0151	0.026
64-ele. array	AEPM	4.98	19.88	75.8	293.18
	Proposed	0.56	1.53	4.7	18.6

array is addressed, the computational time of excitation of virtual array in the first time is about 1300 s, whereas only 0.3 s is required for the proposed solution. The reason for high efficiency of the proposed solution is because the number of array elements has not increased, MC is compensated only by adjusting the excitation. The time comparison indicates that the proposed solution also has the advantages of simplicity and ease of implementation.

IV. CONCLUSION

In this paper, based on the utilization of the NuFFT technique and MCCM, a rapid solution for calculating the radiation pattern of aperiodic arrays when MC effects are taken into consideration, is presented. By compensating the excitation with the MCCM technique, the impacts of MC on the element radiation can be compensated. Furthermore, the NuFFT technique is introduced to accelerate the array pattern calculation. The proposed solution is validated by evaluating the radiation pattern of a planar aperiodic array. In addition, the proposed solution is integrated easily into the PSO algorithm to realize the fast pattern synthesis of aperiodic arrays. Two pattern synthesis examples, including focused beam and flat-top beam patterns with different array numbers, are realized, which indicates that the proposed method can improve the synthesis efficiency and maintain good accuracy simultaneously.

ACKNOWLEDGMENTS

REFERENCES

[1] G. Toso and R. Mailloux, "Guest editorial for the special issue on innovative phased array antennas based on non-regular lattices and overlapped sub-arrays," *IEEE Transactions on Antennas and Propagation*, vol. 62, no. 4, pp. 1546-1548, 2014.

[2] Y.-F. Cheng, W. Shao, S.-J. Zhang, and Y.-P. Li, "An improved multi-objective genetic algorithm for large planar array thinning," *IEEE Transactions on Magnetics*, vol. 52, no. 3, pp. 1-4, 2016.

[3] K. Yang, Z. Q. Zhao, and Q. H. Liu, "Fast pencil beam pattern synthesis of large unequally spaced antenna arrays," *IEEE Transactions on Antennas and Propagation*, vol. 61, no. 2, pp. 627-634, 2013.

[4] P. F. You, Y. H. Liu, X. Huang, L. Zhang, and Q. H. Liu, "Efficient phase-only linear array synthesis including coupling effect by GA-FFT based on least-square active element pattern expansion method," *Electronics Letters*, vol. 51, no. 10, pp. 791-792, 2015.

[5] Y. H. Liu, X. Huang, K. D. Xu, Z. Y. Song, S. W. Yang, and Q. H. Liu "Pattern synthesis of unequally spaced linear arrays including mutual coupling using iterative FFT via virtual active element pattern expansion," *IEEE Transactions on Antennas and Propagation*, vol. 65, no. 8, pp. 3950-3958, 2017.

[6] D. R. Prado, M. Arrebola, M. R. Pino, and F. Las-Heras, "An efficient calculation of the far field radiated by non-uniformly sampled planar fields complying Nyquist theorem," *IEEE Transactions on Antennas and Propagation*, vol. 63, no. 2, pp. 862-865, 2015.

[7] O. Bucci and M. Migliore, "A novel nonuniform fast Fourier transform algorithm and its application to aperiodic arrays," *IEEE Antennas and Wireless Propagation Letters*, vol. 16, pp. 1472-1475, 2017.

[8] A. Capozzoli, C. Curcio, and A. Liseno, "Optimized nonuniform FFTs and their application to array factor computation," *IEEE Transactions on Antennas and Propagation*, vol. 67, no. 6, pp. 3924-3938, 2019.

[9] F. Yang, S. W. Yang, W. J. Long, Y. K. Chen, S. W. Qu, and J. Hu, "A novel 3D-NUFFT method for the efficient calculation of the array factor of conformal arrays," *IEEE Transactions on Antennas and Propagation*, vol. 69, no. 10, pp. 7047-7052, 2021.

[10] Q. H. Liu and N. Nguyen, "An accurate algorithm for nonuniform fast Fourier transforms (NUFFT's)," *IEEE Microwave and Guided Wave Letters*, vol. 8, no. 1, pp. 18-20, 1998.

[11] J. W. Cooley and J. W. Tukey, "An algorithm for the machine calculation of complex Fourier series," *Mathematics of Computation*, vol. 19, no. 90, pp. 297-301, 1965.

[12] W. P. M. N. Keizer, "Fast low-sidelobe synthesis for large planar array antennas utilizing successive fast Fourier transforms of the array factor," *IEEE Transactions on Antennas and Propagation*, vol. 55, no. 3, pp. 715-722, 2007.

[13] W. P. du Plessis, "Efficient computation of array factor and sidelobe level of linear arrays," *IEEE Antennas and Propagation Magazine*, vol. 58, no. 6, pp. 102-114, 2016.

[14] W. P. M. N. Keizer, "Large planar array thinning using iterative FFT techniques," *IEEE Transactions on Antennas and Propagation*, vol. 57, no. 10, pp. 3359-3362, 2009.

[15] L. L. Wang, D. G. Fang, and W. X. Sheng, "Combination of genetic algorithm (GA) and fast Fourier transform (FFT) for synthesis of arrays," *Microwave and Optical Technology Letters*, vol. 37, no. 1, pp. 56-59, 2003.

[16] J. Z. Liu, Z. Q. Zhao, K. Yang, and Q. H. Liu, "A hybrid optimization for pattern synthesis of large antenna arrays," *Progress in Electromagnetics Research-pier*, vol. 145, pp. 81-91, 2014.

[17] Y. J. Miao, F. F. Liu, J. X. Lu, and K. Li, "Synthesis of unequally spaced arrays with uniform excitation via iterative second-order cone programming," *IEEE Transactions on Antennas and Propagation*, vol. 68, no. 8, pp. 6013-6021, 2020.

[18] X. M. Xu, C. Liao, L. Zhou, and F. Peng, "Grating lobe suppression of non-uniform arrays based on position gradient and sigmoid function," *IEEE Access*, vol. 7, pp. 106407-106416, 2019.

[19] D. R. Prado, M. Arrebola, M. R. Pino, and F. Las-Heras, "Application of the NUFFT to the analysis and synthesis of aperiodic arrays," *2017 International Conference on Electromagnetics in Advanced Applications (ICEAA)*, Verona, Italy, pp. 708-711, 2017.

[20] M. Narasimhan and R. S. Rao, "Synthesis of far-field patterns of circular cylindrical arrays," *Microwave and Optical Technology Letters*, vol. 4, no. 5, pp. 196-199, 1991.

[21] H. Steyskal and J. S. Herd, "Mutual coupling compensation in small array antennas," *IEEE Transactions on Antennas and Propagation*, vol. 38, no. 12, pp. 1971-1975, 1990.

[22] J. Rubio, J. F. Izquierdo, and J. Corcoles, "Mutual coupling compensation matrices for transmitting and receiving arrays," *IEEE Transactions on Antennas and Propagation*, vol. 63, no. 2, pp. 839-843, 2014.

[23] J. Corcoles, M. A. Gonzalez, and J. Rubio, "Mutual coupling compensation in arrays using a spherical wave expansion of the radiated field," *IEEE Antennas and Wireless Propagation Letters*, vol. 8, pp. 108-111, 2009.

[24] D. Kelley and W. Stutzman, "Array antenna pattern modeling methods that include mutual coupling effects," *IEEE Transactions on Antennas and Propagation*, vol. 41, no. 12, pp. 1625-1632, 1993.

[25] S. P. Boyd and L. Vandenberghe, *Convex Optimization*, Cambridge, UK, Cambridge University Press, 2004.

[26] D. W. Boeringer and D. H. Werner, "Particle swarm optimization versus genetic algorithms for phased array synthesis," *IEEE Transactions on Antennas and Propagation*, vol. 52, no. 3, pp. 771-779, 2004.

[27] N. Jin and Y. Rahmat-Samii, "Advances in particle swarm optimization for antenna designs: Real-number, binary, single-objective and multiobjective implementations," *IEEE Transactions on Antennas and Propagation*, vol. 55, no. 3, pp. 556-567, 2007.

[28] W.-C. Liu, "Design of a multiband CPW-fed monopole antenna using a particle swarm optimization approach," *IEEE Transactions on Antennas and Propagation*, vol. 53, no. 10, pp. 3273-3279, 2005.

[29] Y. H. Liu, Z.-P. Nie, and Q. H. Liu, "A new method for the synthesis of non-uniform linear arrays with shaped power patterns," *Progress in Electromagnetics Research*, vol. 107, pp. 349-363, 2010.

Fan Peng received his Bachelor's degree in applied physics from the Chengdu University of Information and Technology (CUIT), Chengdu, China. In 2016, he entered Southwest Jiaotong University to study for Ph.D. degree in electromagnetic field and electromagnetic waves. His current research includes wide beam antenna, phased array and array synthesis.

Cheng Liao received his Ph.D. degree in electromagnetic fields and microwave technology from the University of Electronic Science and Technology of China, Chengdu, China, in 1995.

From 1997 to 1998, he was a Visiting Scholar with the City University of Hong Kong, Kowloon Tong, Hong Kong. In 1998, he became a Professor with Southwest Jiaotong University, Chengdu. His research interests include computational electromagnetics, electromagnetic compatibility, and antenna theory and technology.

YouFeng Cheng was born in Anqing, Anhui, China, in 1989. He received his Ph.D. degree in radio physics from the University of Electronic Science and Technology of China (UESTC), Chengdu, China, in 2018.

In 2017, he joined the Mechanical Engineering Department, University of Houston, Houston, TX. USA, as a Visiting Scholar. In 2018, he joined Southwest Jiaotong University (SWJTU), Chengdu. His current research interests include phased arrays, reconfigurable antennas, and evolutionary algorithms.

Ju Feng received her Ph.D. degree in electromagnetic field and microwave technology from Southwest Jiaotong University, Chengdu, China, in 2014.

She is currently an Associate Professor at the Institute of Electromagnetic Field and Microwave Technology, Southwest Jiaotong University. Her major research interests include antenna theory and design, computational electromagnetics, and electromagnetic wave propagation.

Sidu Wang received his Bachelor's scholar degree in electronic and information engineering from the Chengdu University of Information and Technology (CUIT), Chengdu, China. In 2015, he worked at the Civil Aviation Flight Univerity of China (CAFUC), Guanghan, China. His current research includes signal communication, navigation, radar, and aviation safety management.